

## DETERMINATION OF LIMITING FLUX AND THRESHOLD PRESSURE IN STIRRED ULTRAFILTRATION OF COLLOIDAL SUSPENSIONS

Goran T. VLADISAVLJEVIC<sup>1</sup> and Vladeta Lj. PAVASOVIC<sup>2</sup>

*Institute of Food Technology and Biochemistry, Faculty of Agriculture, Belgrade University,  
P.O.Box 127, 11081 Belgrade-Zemun, Yugoslavia; e-mail: <sup>1</sup>gtyvladis@afrodita.rcub.bg.ac.yu.,  
<sup>2</sup>zoya@rt270.vin.bg.ac.yu*

Received August 5, 1996

Accepted May 12, 1997

The stationary permeate flux during ultrafiltration of colloidal suspensions reaches a limiting value,  $J_l$ , at high pressure differences. According to the gel polarization model employed here, the existence of this limiting flux is a consequence of gelation of the solution at the membrane–solution interface. The limiting permeate flux,  $J_l$ , can easily be determined from experimental data by plotting  $\Delta p/J_s$  against  $\Delta p$ . Furthermore, the membrane resistance at zero pressure difference,  $R_m^0$ , and the pressure difference necessary to reach 95 per cent of the limiting flux, *i.e.* the threshold pressure,  $\Delta p_t$ , may be calculated, too. The agreement between the model and experimental data is satisfactory. The laboratory-made silica sol consisting of uniform spherical particles with a surface average diameter of 18 nm was selected as a working fluid throughout this study.

**Key words:** Ultrafiltration; Limiting flux; Membrane resistance; Silica sol; Threshold pressure.

Ultrafiltration is a pressure-driven membrane process by which macrosolutes in the range of 2 to 50 nm or 500 to 300 000 g mol<sup>-1</sup> are separated from the solvent and other smaller constituents. The separation of various species is achieved by the selective permeation through the membrane. When a solute is fully rejected by the membrane, the stationary permeate flux,  $J_s$ , is given by<sup>1</sup>

$$J_s = (dV/dt)_s (1/A_m) = K \ln (C_m/C_b) , \quad (1)$$

where  $(dV/dt)_s$  is the slope of the permeate volume *vs* time plot at stationary state,  $A_m$  is the effective cross-sectional membrane area,  $K = D/\delta$  is the mass transfer coefficient,  $\delta$  is the boundary layer thickness,  $D$  is the particle diffusion coefficient, and  $C_m$  and  $C_b$  are the concentration of particles at the surface of the membrane and in the bulk solution, respectively.

The diffusion coefficient for non-interacting particles (in dilute solutions) can be calculated by the Stokes–Einstein relationship<sup>2</sup>

$$D = kT/(3\pi\eta d_s) , \quad (2)$$

where  $k$  is the Boltzman constant,  $T$  is the thermodynamic temperature of solution,  $\eta$  is the solvent viscosity, and  $d_s$  is the surface average diameter of particles.

According to the gel layer theory<sup>1</sup>,  $J_s$  increases with  $\Delta p$  only until  $C_m$  reaches a  $C_g$  value, high enough for the solution at the membrane surface to turn into a gel. The limiting permeate flux,  $J_l$ , is obtained by substituting  $C_m = C_g$  into Eq. (1) (refs<sup>1,3</sup>)

$$J_l = K \ln (C_g/C_b) \quad (3)$$

Equation (3) shows that the limiting permeate flux depends on the feed solution physico-chemical properties ( $D$  and  $C_g$ ), the concentration of particles in the bulk solution, and the hydrodynamic conditions existing within the boundary layer, but is independent of the membrane resistance. The most effective way to increase the limiting permeate flux is to reduce the boundary layer thickness by increasing either the stirrer speed (for magnetically driven stirred cells) or the flow velocity inside the feed channel (for recirculating systems). The stationary permeate flux can also be expressed by the resistances-in-series relationship<sup>4,5</sup>

$$J_s = \Delta p / (R_m + R_g) \eta \quad (4)$$

where  $\Delta p$  denotes the total pressure difference,  $R_m$  and  $R_g$  the resistance of the membrane and the gel layer, respectively, and  $\eta$  the permeate viscosity. It is worth mentioning here that Eqs (1) and (4) must give the same result under the same conditions.

The aim of this work is to propose a simple method for the determination of the limiting permeate flux, the membrane resistance, and the threshold pressure in stirred ultrafiltration of colloidal suspensions. The term threshold pressure will be referred to the pressure difference at which the permeate flux is 95 per cent of its limiting value. The method proposed here is based on the knowledge of the experimental  $J_s$ - $\Delta p$  dependencies obtained by stirred ultrafiltration below the threshold pressure. Contrary to the model proposed by Aimar and Sanchez<sup>6</sup>, our model does not require the knowledge of the system geometry, the hydrodynamic conditions, the bulk concentration of the dispersed phase or the physico-chemical properties of the feed solution.

## EXPERIMENTAL

The experiments were performed in a Sartorius batch cell, model SM 16526, with a capacity of 200 cm<sup>3</sup>, a membrane diameter of 47 mm and an effective membrane area of 12.5 cm<sup>2</sup>. The cell has a removable plastic jacket, so that the fluid to be ultrafiltrated can be warmed or cooled by passing water from a thermostat bath through the jacket. All the experiments were performed with one and the

same membrane produced by Amicon, model Diaflo PM-10. This membrane is made of polysulfone with a nominal molecular weight cut-off of 10 000 g mol<sup>-1</sup> and an apparent pore diameter of 3.8 nm.

An experiment commenced with the introduction of 100 cm<sup>3</sup> of distilled water or silica sol into the cell with membrane in position. The cell was then quickly pressurized to the operating pressure by nitrogen gas. Each experiment was performed until 10–12 cm<sup>3</sup> of the permeate was collected, which took from 15 to 190 min at  $T = 293\text{--}323\text{ K}$ ,  $\Delta p = 50\text{--}350\text{ kPa}$  and  $C_b = 10\text{--}24\text{ kg m}^{-3}$ . Stirring was provided by a built-in teflon-coated stirring bar, suspended 1 mm from the upper surface of the membrane. The stirrer speed was controlled by varying the speed of the magnetic stirring table on which the cell rested. The stirrer speed was fixed at 400 revolutions per minute to prevent the formation of a significant vortex in the cell. The mass of permeate collected was measured as a function of time on a Sartorius digital balance with an accuracy of  $\pm 0.01\text{ g}$ . Since the particles were completely retained by the membrane, the permeate density and viscosity was taken as equal to pure water density and viscosity.

Silica sol consisting of uniform spherical particles with a surface average diameter of 18 nm and a specific surface area of 151 m<sup>2</sup> g<sup>-1</sup> was chosen as a colloidal suspension. It was made by passing relatively dilute sodium silicate solution through a column of hydrogen form of an acid ion-exchange resin (Amberlite IR 120), according to the procedure described in the literature<sup>7</sup>.

## RESULTS AND DISCUSSION

### Membrane Resistance

Before the first experiment, the membrane was washed out by distilled water at the pressure difference of 300 kPa to remove the protective layer of glycerol. After washing out, the membrane resistance,  $R_m$ , was obtained from the experiments with distilled water permeation using Eq. (4), in which  $R_g$  was taken as zero. It was found that  $R_m$  increases linearly with  $\Delta p$  (Fig. 1):

$$R_m = R_m^0 + \beta \Delta p \quad , \quad (5)$$

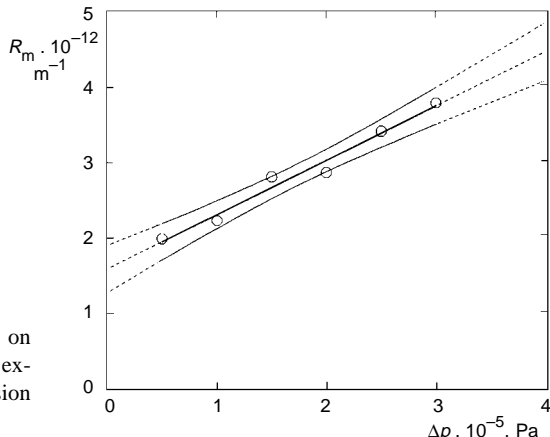


FIG. 1  
Effect of applied pressure difference on membrane resistance at 293 K:  $\circ$  experimental points, — linear regression line, Eq. (5) ( $r = 0.9874$ )

where  $R_m^0 = (1.6 \pm 0.3) \cdot 10^{12} \text{ m}^{-1}$  is the membrane resistance at zero pressure difference and  $\beta = (7.2 \pm 1.6) \cdot 10^{-6} \text{ m N}^{-1}$  is the increase in  $R_m$  due to the increase in  $\Delta p$  of 1 Pa (for an incompressible membrane  $\beta = 0$ ). The fact that an Amicon Diaflo PM-10 membrane is significantly compressible is also reported in our previous paper<sup>8</sup>.

### Determination of $J_1$ and $R_m^0$ from Relationship Between $J_s$ and $\Delta p$

Typical data for stirred ultrafiltration of silica sol are plotted as the  $V-t$  dependencies in Figs 2 and 3. The permeate volume collected at any time increased strongly with decreasing bulk concentration and with increasing temperature. The points at which the steady-state is established are indicated by small arrows. The values of  $J_s$  were obtained from the slopes of the linear regions of the  $V$  vs  $t$  plots, situated on the right side of these arrows. The stationary flux vs pressure difference plots are shown in Fig. 4. It is

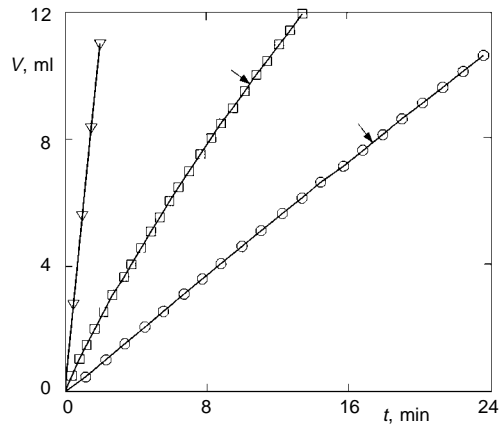


FIG. 2

Effect of bulk silica concentration on permeate volume vs time profiles at  $\Delta p = 2.5 \cdot 10^5 \text{ Pa}$  and  $T = 293 \text{ K}$ :  $\nabla C_b = 0 \text{ kg m}^{-3}$ ,  $\square C_b = 24 \text{ kg m}^{-3}$ ,  $\circ C_b = 52 \text{ kg m}^{-3}$

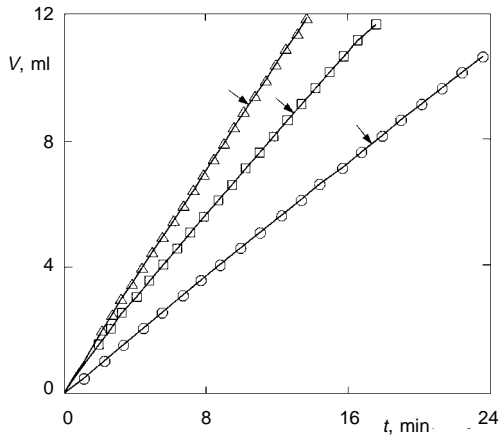


FIG. 3

Effect of temperature on permeate volume vs time profiles at  $\Delta p = 2.5 \cdot 10^5 \text{ Pa}$  and  $C_b = 52 \text{ kg m}^{-3}$ :  $\circ T = 293 \text{ K}$ ,  $\square T = 308 \text{ K}$ ,  $\Delta T = 323 \text{ K}$

evident that at the same pressure difference, the stationary flux increased with decreasing  $C_b$  and with increasing temperature (due to an increase in  $D$ ), as predicted from Eq. (1). Applying Eqs (4) and (5), one obtains:

$$\lim_{\Delta p \rightarrow \infty} J_s = J_l = \Delta p / (\beta \Delta p + R_g \eta) \quad (6)$$

since  $R_m^0 \ll \beta \Delta p + R_g$  when  $\Delta p \rightarrow \infty$ . On using Eqs (5) and (6), Eq. (4) can be rewritten:

$$\Delta p / J_s = \eta R_m^0 + \Delta p / J_l. \quad (7)$$

Equation (7) predicts that a plot of  $\Delta p / J_s$  vs  $\Delta p$  will give a straight line with a slope of  $1/J_l$  and an intercept of  $\eta R_m^0$ . Thus, such plot yields  $J_l$  from the slope and  $R_m^0$  from the intercept.

TABLE I

Membrane resistances at zero pressure difference,  $R_m^0$ , parameters of Eq. (8),  $b$  and  $J_l$ , and threshold pressures,  $\Delta p_t$ , for stirred ultrafiltration of silica sol<sup>a</sup>

| $T, K$ | $C_b, \text{kg m}^{-3}$ | $R_m^0 \cdot 10^{-12} \text{ m s}^{-1}$ | $J_l \cdot 10^6 \text{ m s}^{-1}$ | $b \cdot 10^5 \text{ Pa}^{-1}$ | $\Delta p_t \cdot 10^{-5} \text{ Pa}$ | $r$     | $n$ |
|--------|-------------------------|---|-----------------------------------|--------------------------------|---------------------------------------|---------|-----|
| 293    | 10                      | $1.9 \pm 0.6$                           | 14.1                              | 3.77                           | 5.0                                   | 0.9998  | 5   |
| 293    | 24                      | $0.86 \pm 2.7$                          | 10.4                              | 11.2                           | 1.7                                   | 0.9948  | 6   |
| 323    | 10                      | $2.1 \pm 0.3$                           | 25.2                              | 3.43                           | 5.5                                   | >0.9999 | 4   |
| 323    | 24                      | $2.5 \pm 1.4$                           | 16.9                              | 4.38                           | 4.3                                   | 0.9989  | 6   |

<sup>a</sup>  $J_l$  and  $R_m^0$  were derived from the plots in Fig. 5, whereas  $b$  and  $\Delta p_t$  were calculated by means of Eq. (9).

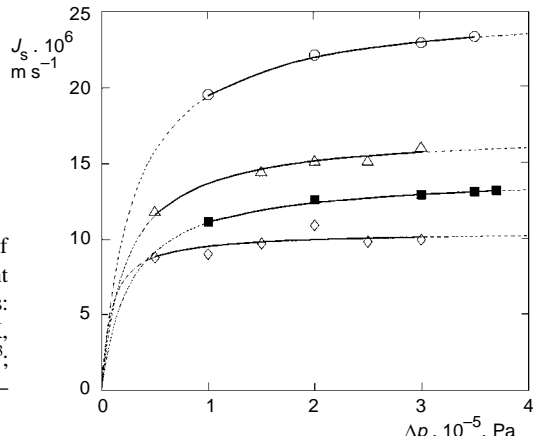


FIG. 4

Stationary permeate flux as a function of applied pressure difference at two different temperatures and bulk silica concentrations:  
 ○  $T = 323 \text{ K}$ ,  $C_b = 10 \text{ kg m}^{-3}$ ; Δ  $T = 323 \text{ K}$ ,  $C_b = 24 \text{ kg m}^{-3}$ ; ■  $T = 293 \text{ K}$ ,  $C_b = 10 \text{ kg m}^{-3}$ ;  
 ◇  $T = 293 \text{ K}$ ,  $C_b = 24 \text{ kg m}^{-3}$ ;  
 — lines drawn according to Eq. (8)

The values of  $J_l$  and  $R_m^0$  listed in Table I were determined from the  $\Delta p/J_s$  vs  $\Delta p$  plots shown in Fig. 5. Calculations were done using a linear regression analysis program and the correlation coefficients thus obtained represent the accuracy of the data fit to a straight line. It follows from Table I that the limiting permeate flux,  $J_l$ , decreases with increasing  $C_b$  and with decreasing temperature, which is consistent with Eq. (3). Except for  $C_b = 24 \text{ kg m}^{-3}$  and  $T = 293 \text{ K}$ , the values of  $R_m^0$  are higher than  $(1.6 \pm 0.3) \cdot 10^{12} \text{ m}^{-1}$ , following from Eq. (5) for the same membrane on first usage. This can be attributed to an irreversible pore blocking by silica particles during the experiments and possible deposition of an adsorption layer on the membrane surface, which cannot be removed when the pressure is released. It may be concluded that the membrane became fouled with silica particles and that membrane cleaning with distilled water between the individual runs was unable to restore completely the initial membrane resistance.

The dependences of  $J_s$  on  $\Delta p$  given in Fig. 4 can be described by an expression similar to the Langmuir isotherm<sup>9</sup>:

$$J_s = J_l b \Delta p / (1 + b \Delta p) , \quad (8)$$

where  $b$  and  $J_l$  are independent of  $\Delta p$  but vary with the bulk concentration and temperature. Substituting  $J_s = J_l/2$  into Eq. (8) gives  $b = 1/\Delta p_h$ . Therefore, the physical meaning of the parameter  $b$  is that it is the reciprocal of pressure difference for which the stationary flux is one half of the limiting flux. The solid lines in Fig. 4 are drawn according to Eq. (8) by using the values of  $b$  and  $J_l$  listed in Table I. It is obvious that these lines agree well with the experimental data. At the values of  $b \Delta p$  much lower than unity ( $J_s \approx J_l b \Delta p$ ), the stationary flux is a linear function of the pressure difference and the proportionality constant is  $J_l b = 1/(\eta R_m^0)$ . It is a pure filtration or Darcy's law region

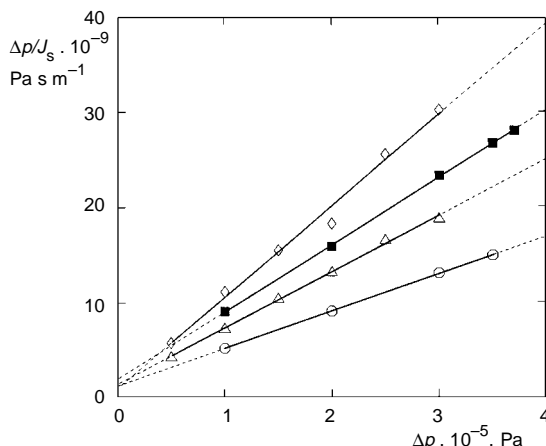


FIG. 5  
Relationship between  $\Delta p/J_s$  and  $\Delta p$  obtained by using experimental data from Fig. 4; keys are the same as in Fig. 4

where the stationary flux is controlled by the membrane resistance and the pressure difference. However, when the values of  $b \Delta p$  are much higher than unity ( $J_s \approx J_l$ ), the pressure difference and the membrane resistance have no influence on the stationary flux. Under these conditions, Eq. (3) holds and the stationary flux is limited by the mass-transfer conditions in the boundary layer: we are in the ultrafiltration region. The same type of flux-pressure behaviour as predicted by Eq. (8), *i.e.* the existence of a limiting flux at high pressure differences and a linear flux-pressure relationship for small  $\Delta p$  values, was observed by Do and Elhassadi<sup>10</sup> for the stirred ultrafiltration of BSA, by Nabetani *et al.*<sup>11</sup> for the ultrafiltration of ovalbumin in a crossflow apparatus, and by Song *et al.*<sup>12</sup> for the ultrafiltration of non-interacting particles in theoretically modelled crossflow systems.

#### Verification of Gel Polarization Model

Equation (3) indicates that the  $J_l$  vs  $\ln(C_b)$  plot will give a straight line with a slope equal to  $(-K)$  and an intercept on abscissa of  $\ln(C_g)$ . Two such lines concerning the

TABLE II

Effect of temperature on mass transfer in boundary layer formed during stirred ultrafiltration of silica sol

| $T, K$ | $C_g, \text{kg m}^{-3}$ | $K \cdot 10^6$<br>$\text{m s}^{-1}$ | $D \cdot 10^{11}$<br>$\text{m}^2 \text{s}^{-1}$ | $\delta \cdot 10^6, \text{m}$ | $r$    |
|--------|-------------------------|-------------------------------------|---|-------------------------------|--------|
| 293    | 360                     | 3.8                                 | 2.4   | 6                             | -0.966 |
| 323    | 364                     | 6.7                                 | 4.8   | 7                             | -0.974 |

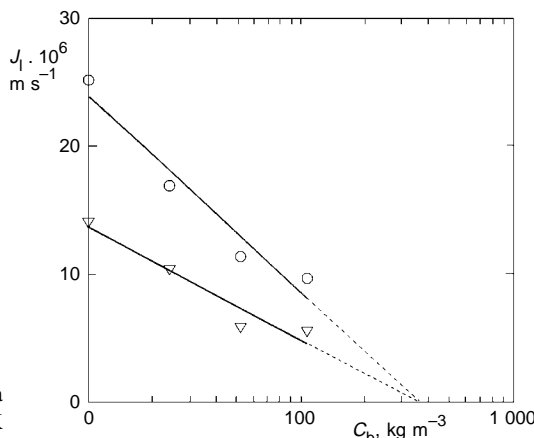


FIG. 6  
Variation of limiting flux with bulk silica concentration:  $\nabla T = 293 \text{ K}$ ,  $\circ T = 323 \text{ K}$

stirred ultrafiltration of silica sol at 293 and 323 K are presented in Fig. 6. It is obvious that the slope of the  $J_1$  vs  $\ln(C_b)$  plot (*i.e.* the mass transfer coefficient) is higher at higher temperature. However, the intercept on the abscissa is almost identical in both cases indicating that the gel concentration,  $C_g$ , is independent of temperature. The arithmetic mean of the  $C_g$  values of  $362 \text{ kg m}^{-3}$  for 293 and 323 K is fairly close to the  $428 \text{ kg m}^{-3}$  value reported by Fane<sup>4</sup> for commercial silica sols produced by Syton, type X30 and W30, but much lower than the value of  $1\,220 \text{ kg m}^{-3}$  reported by Chudacek and Fane<sup>13</sup> for Syton X30 sol. The reason for these discrepancies may lie in the fact that the mean particle diameters and the pH values of silica sols used in these studies were different to those in our experiments.

The  $C_g$ ,  $K$ ,  $D$  and  $\delta$  values are listed in Table II. The  $K$  and  $C_g$  values were determined from the slope and the intercept on the abscissa in Fig. 6, respectively. The silica particle diffusion coefficients were calculated by means of Eq. (2) and the  $\delta$  values were determined as  $\delta = D/K$ . However, it must be noted that Eq. (3) strictly applies to particles in dilute suspensions so that it is not wholly successful in predicting the diffusion coefficient in the boundary layer where high particle concentrations are encountered. Because of uncertainty in the value of  $D$ , the boundary layer thickness in Table II are only approximate. It should be pointed out here that the boundary layer thickness,  $\delta$ , is not significantly affected by the temperature.

#### Threshold Pressure

When  $J_s/J_1 \geq 0.95$ , the stationary permeate flux can be regarded as the limiting flux so that the pressure difference necessary to reach 95 per cent of the limiting flux will be referred to as the threshold pressure,  $\Delta p_t$ . Substituting  $J_s = 0.95J_1$  into Eq. (7) and the application of Eqs (8) and (3) gives:

$$\Delta p_t = 19/b = 19R_m^0 \eta J_1 = 19R_m^0 \eta K \ln(C_g/C_b) . \quad (9)$$

Equation (9) shows that the threshold pressure,  $\Delta p_t$ , increases with increasing the membrane resistance, as shown experimentally by Michaels<sup>1</sup> and Nabetani *et al.*<sup>10</sup> and theoretically by Aimar and Sanchez<sup>11</sup> within the framework of the osmotic pressure theory. The analysis of our previously reported data<sup>8</sup> and Table II suggests that the  $R_m^0$ ,  $C_g$  and  $\delta$  are virtually independent of temperature, and  $D$  is proportional to the ratio  $T/\eta$  according to Bird *et al.*<sup>2</sup>, from which it follows that  $\Delta p_t$  is proportional to the thermodynamic temperature. However, the validity of this assumption is only confirmed for  $C_b = 10 \text{ kg m}^{-3}$  (Table I).

## CONCLUSIONS

The stationary permeate flux for stirred ultrafiltration increases less than linearly with the applied pressure difference and reaches a constant value at high pressure differences. This constant flux is called "limiting flux" and may be determined from the slope of the  $\Delta p/J_s$  vs  $\Delta p$  plot (Fig. 5). The limiting fluxes for stirred ultrafiltration of silica sol determined by using this procedure are in qualitative agreement with Michaelis' formula (3). The intercept of the  $\Delta p/J_s$  vs  $\Delta p$  plot enables the membrane resistance at zero applied pressure,  $R_m^0$ , to be obtained. Typically, the  $R_m^0$  values determined by using the model are higher than that for the same membrane on first usage, determined from the distilled water permeability data, which can be attributed to an irreversible membrane fouling not allowed for in our model. The applied pressure necessary to reach 95 per cent of the limiting flux,  $\Delta p_t$ , increases with increasing  $R_m^0$  and temperature, and with decreasing  $C_b$ . However, the temperature does not affect the concentration of silica particles in the gel layer and the boundary layer thickness.

## SYMBOLS

|              |   |
|--------------|---|
| $A_m$        | effective cross-sectional membrane area, $\text{m}^2$   |
| $b$          | constant in Eq. (6), $\text{Pa}^{-1}$   |
| $C_b$        | concentration of particles in bulk solution, $\text{kg m}^{-3}$   |
| $C_g$        | concentration of particles in gel layer, $\text{kg m}^{-3}$   |
| $C_m$        | concentration of particles at the membrane surface, $\text{kg m}^{-3}$  |
| $D$          | particle diffusion coefficient, $\text{m}^2 \text{s}^{-1}$  |
| $d_s$        | surface average diameter of particles, $\text{m}$   |
| $J_l$        | limiting permeate flux, $\text{m s}^{-1}$   |
| $J_s$        | stationary permeate flux, $\text{m s}^{-1}$   |
| $K$          | mass transfer coefficient, $\text{m s}^{-1}$  |
| $k$          | Boltzman constant ( $1.380 \cdot 10^{-23} \text{ J K}^{-1}$ )   |
| $m_x$        | arithmetic mean of the $x_i$ values for the regression calculations   |
| $m_y$        | arithmetic mean of the $y_i$ values for the regression calculations   |
| $n$          | number of points for the regression calculations  |
| $\Delta p$   | pressure difference, $\text{Pa}$  |
| $\Delta p_h$ | pressure difference at which $J_s = J_l/2$ , $\text{Pa}$  |
| $\Delta p_t$ | pressure difference necessary to reach 95 per cent of the limiting flux, the so-called threshold pressure, $\text{Pa}$                |
| $R_g$        | gel resistance, $\text{m}^{-1}$   |
| $R_m$        | membrane resistance, $\text{m}^{-1}$  |
| $R_m^0$      | membrane resistance at zero pressure difference, $\text{m}^{-1}$  |
| $r$          | correlation coefficient, $r = (\sum_{i=1}^n x_i y_i - nm_x m_y) / [(\sum_{i=1}^n x_i^2 - nm_x^2)(\sum_{i=1}^n y_i^2 - nm_y^2)]^{1/2}$ |
| $T$          | thermodynamic temperature, $\text{K}$   |
| $t$          | time, $\text{s}$  |
| $V$          | permeate volume, $\text{m}^3$   |
| $\beta$      | constant in Eq. (5), $\text{m N}^{-1}$  |

---

|          |                                       |
|----------|---------------------------------------|
| $\delta$ | boundary layer thickness, m           |
| $\eta$   | solvent (or permeate) viscosity, Pa s |

## REFERENCES

1. Michaels A. S.: *Chem. Eng. Prog.* **64**, 31 (1968).
2. Bird R. B., Stewart W. E., Lightfoot E. N.: *Transport Phenomena*, Chap. 16, p. 495. Wiley, New York 1966.
3. Porter M. C.: *Ind. Eng. Chem., Prod. Res. Dev.* **11**, 234 (1972).
4. Fane A. G.: *J. Membr. Sci.* **20**, 249 (1984).
5. Kim K., Chen V., Fane A. G.: *J. Colloid Interface Sci.* **155**, 347 (1993).
6. Aimar P., Sanchez V.: *Ind. Eng. Chem., Fundam.* **25**, 789 (1986).
7. Milonjic S. K., Kopecni M. M., Ilic Z. E.: *Bull. Soc. Chem. Belgrade* **48**, 351 (1983).
8. Vladisavljevic G. T., Milonjic S. K., Pavasovic V. Lj.: *J. Colloid Interface Sci.* **176**, 491 (1995).
9. Vladisavljevic G. T., Milonjic S. K., Nikolic D., Pavasovic V. Lj.: *J. Membr. Sci.* **66**, 9 (1992).
10. Do D. D., Elhassadi A. A.: *J. Membr. Sci.* **25**, 113 (1985).
11. Nabetani H., Nakajima M., Watanabe A., Nakao S., Kimura S.: *AIChE J.* **36**, 907 (1990).
12. Song L., Elimelech M.: *J. Chem. Soc., Faraday Trans.* **91**, 3389 (1995).
13. Chudacek M. W., Fane A. G.: *J. Membr. Sci.* **21**, 145 (1984).